



中国科学技术大学

University of Science and Technology of China

# Direct observation of the dead-cone effect in quantum chromodynamics

ALICE Collaboration. Direct observation of the dead-cone effect in quantum chromodynamics. Nature 605, 440–446 (2022). <https://doi.org/10.1038/s41586-022-04572-w>

高能物理实验数据分析 期末报告

张原 SA22004065

# Outline

- **Introduction**
- **Analysis method**
- **Result**
- **Conclusion**

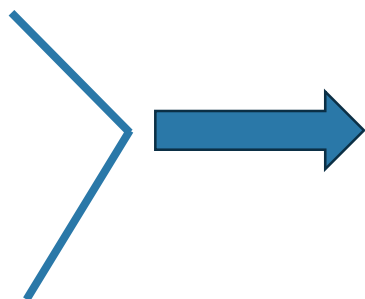
# Introduction

- 量子色动力学 (QCD) 是描述强相互作用的基本理论。
  - 渐近自由
  - 夸克禁闭



实验上可观测到的粒子都是色中性的

在高能粒子碰撞实验中，在大动量转移的过程中会产生一些夸克和胶子，这些夸克和胶子会经过一系列辐射，产生更多夸克和胶子，称为parton shower。



Parton shower 会经过强子化生成大量末态强子。



这些在相近方向上高速飞行的强子束被称作jet

依据QCD理论，质量为 $m$ 、能量为 $E$ 的辐射体辐射胶子时，在相对其运动方向 $m/E$ 角度范围内辐射会被压低，即**Dead-cone effect**

# Introduction

- Dead-cone effect对于轻夸克影响很小，但对于重味夸克，例如c 和b 夸克（质量分别约为1.28GeV和4.18GeV），会有相对较明显的影响。
- 但dead-cone effect之前从未被直接观测到，因为有一些困难：
  - Dead cone角范围内会被其他粒子，例如衰变产物或是无关背景填充。
  - 难以精确得到子粒子的分散角。



**Declustering method**

ALICE Collaboration. Direct observation of the dead-cone effect in quantum chromodynamics. Nature 605, 440–446 (2022).

<https://doi.org/10.1038/s41586-022-04572-w>

# Analysis method

## ➤ Jet reconstruction

**Generalised- $k_t$  algorithm.** Most of the recombination algorithms used in the context of hadronic collisions belong to the family of the *generalised- $k_t$  algorithm* [56] which clusters jets as follows.

1. Take the particles in the event as our initial list of objects.
2. From the list of objects, build two sets of distances: an *inter-particle distance*

$$d_{ij} = \min(p_{t,i}^{2p}, p_{t,j}^{2p}) \Delta R_{ij}^2, \quad (3.1)$$

where  $p$  is a free parameter and  $\Delta R_{ij}$  is the geometric distance in the rapidity-azimuthal angle plane (Eq. (2.33)), and a *beam distance*

$$d_{iB} = p_{t,i}^{2p} R^2, \quad (3.2)$$

with  $R$  a free parameter usually called the *jet radius*.

3. Iteratively find the smallest distance among all the  $d_{ij}$  and  $d_{iB}$ 
  - If the smallest distance is a  $d_{ij}$  then objects  $i$  and  $j$  are removed from the list and recombined into a new object  $k$  (using the recombination scheme) which is itself added to the list.
  - If the smallest is a  $d_{iB}$ , object  $i$  is called a *jet* and removed from the list.

Go back to step 2 until all the objects in the list have been exhausted.

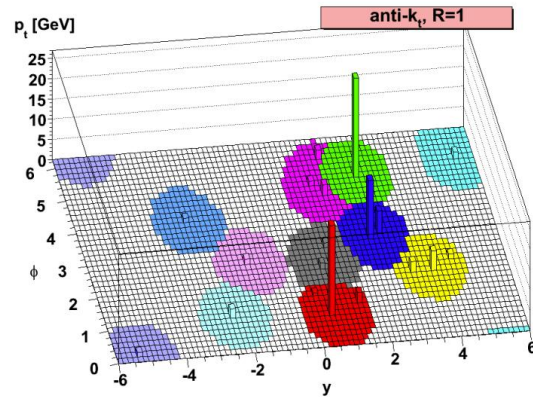
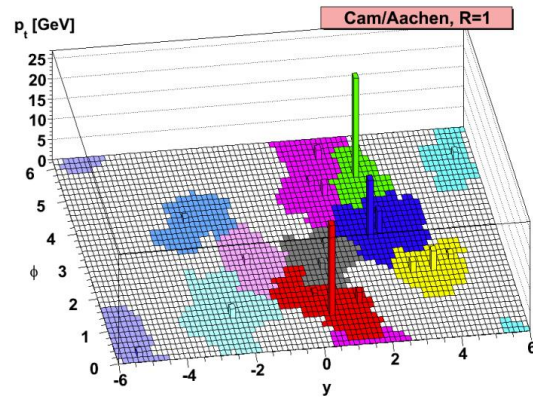
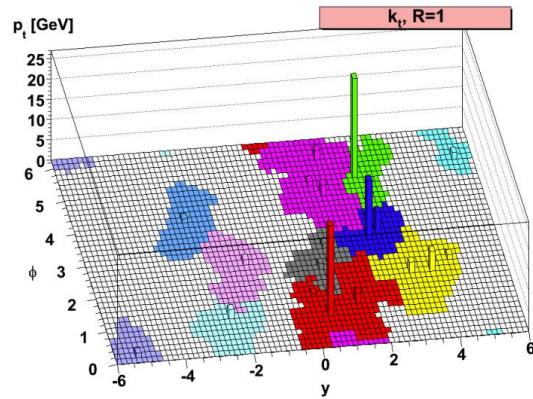
$$\Delta R_{ij}^{(\text{detector})} = \sqrt{(\phi_i - \phi_j)^2 + (\eta_i - \eta_j)^2}.$$

arXiv:1901.10342

Two free parameters:  $R$  and  $p$   
Usual values for  $R$ : 0.4, 0.6, 1.0

- $k_t$  algorithm:  $p=1$
- Cambridge/Aachen algorithm:  $p=0$
- Anti- $k_t$  algorithm:  $p = -1$

# Analysis method

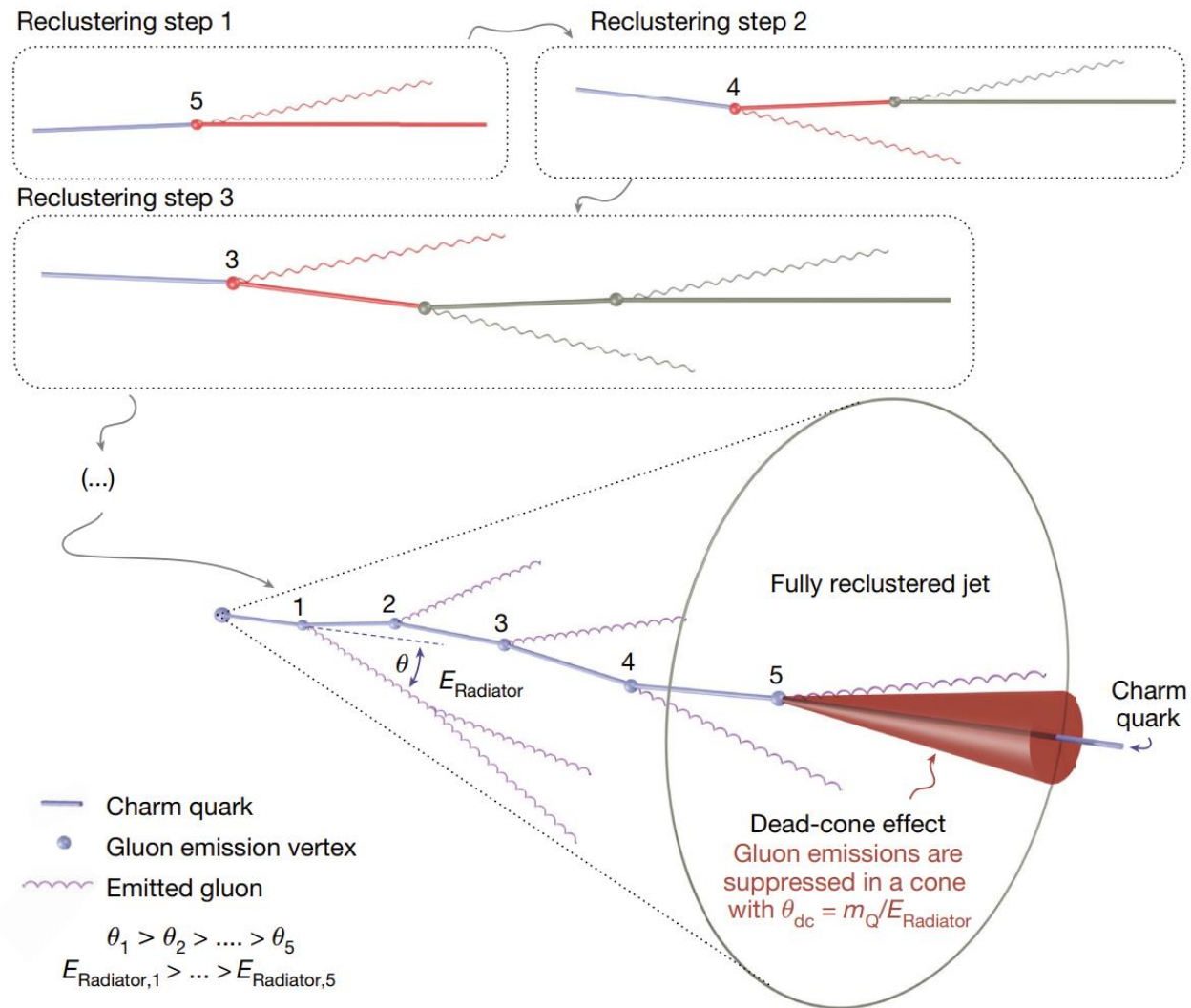


- $k_T$  algorithm: soft emissions 优先组合, 符合微扰QCD, 但容易受事例中其他 soft radiation的影响。
- Cam/Aachen algorithm: 仅考虑几何距离, 更少的受到soft background的影响。
- anti- $k_T$  algorithm: hard particle 优先组合, 然后再聚体周边的soft particle, 受soft background的影响最小。是实验中最常用的方法。

# Analysis method

## ➤ Recluster and decluster:

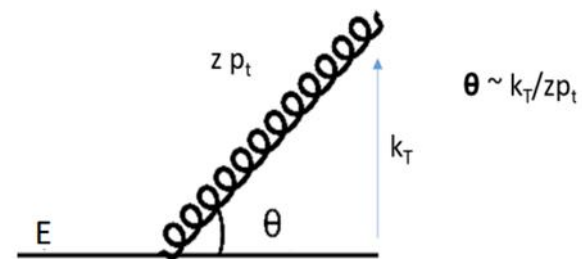
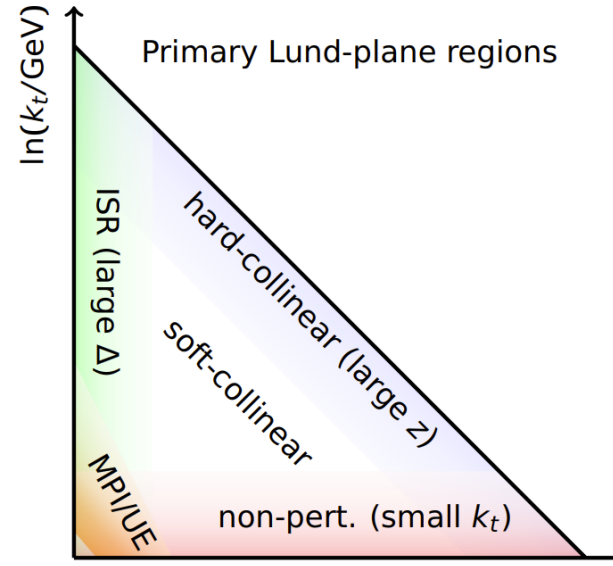
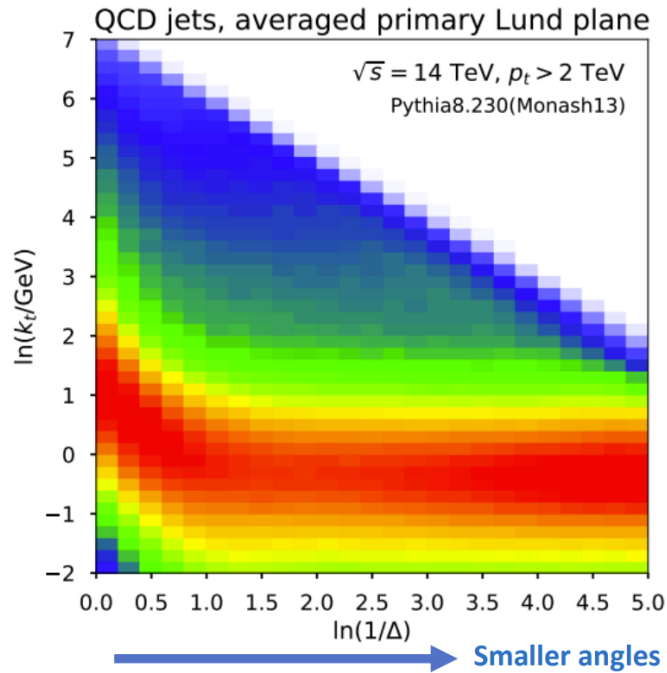
- 先用anti-kT的方法做jet finding
- 再用Cam/Aachen对jet内的组分做recluster。
- 将recluster中partons结合的顺序展开做decluster，就可得到夸克在jet中辐射的顺序



# Analysis method

## ➤ Lund map

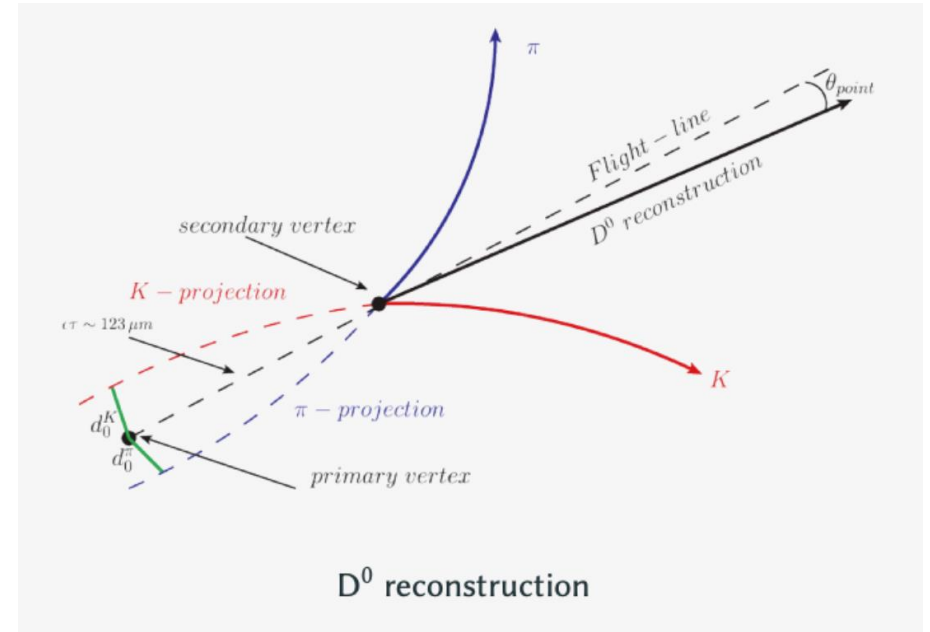
F. A. Dreyer, G. P. Salam and G. Soyez, JHEP 1812, 064



- $E$  : Total energy of the radiator
- $\theta$  : Angle between daughter prongs
- $k_T$  : Splitting scale

# Analysis method

- $D^0 \rightarrow K^\pm \pi^\mp$  with a branching ratio of 3.89%
- $D^0$  candidates are reconstructed through:
  - ❖ PID of K and  $\pi$
  - ❖ Topological cuts on the secondary vertex
- K and  $\pi$  pairs are replaced by the  $D^0$  candidate prior to jet finding
  - ❖ Mitigates against cases where the angle between the daughters is larger than the jet radius – better jet energy resolution
  - ❖  $D^0$  candidate can be tracked through the splitting tree
- Jet finding is performed independently for each  $D^0$  candidate in an event
- Jets are clustered using the anti- $k_T$  algorithm with  $R=0.4$
- The jets are reclustered with the Cambridge-Aachen algorithm in exclusive mode
- $5 < p_{T,jet} < 50 \text{ GeV}/c$        $2 < p_{T,D} < 36 \text{ GeV}/c$        $|\eta_{jet}| < 0.5$

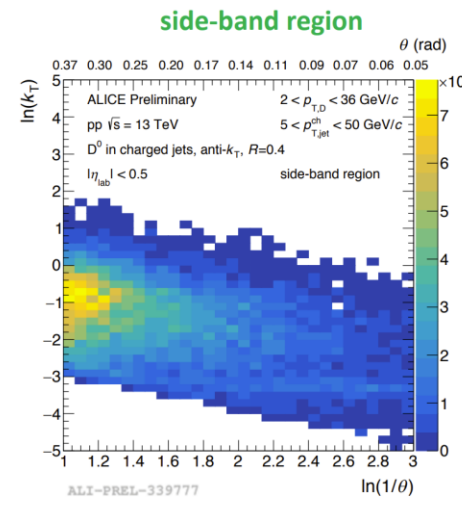
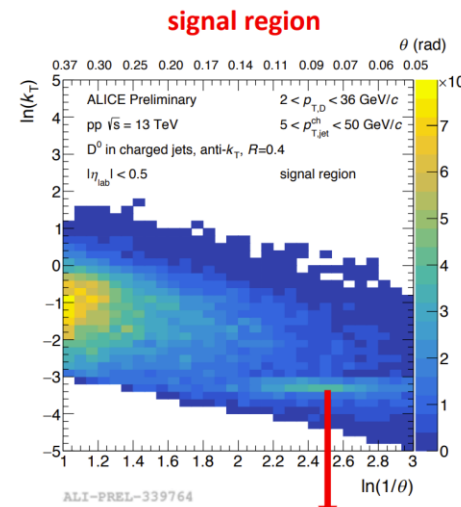
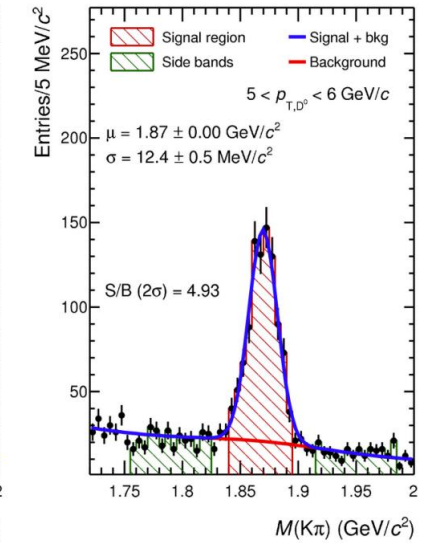
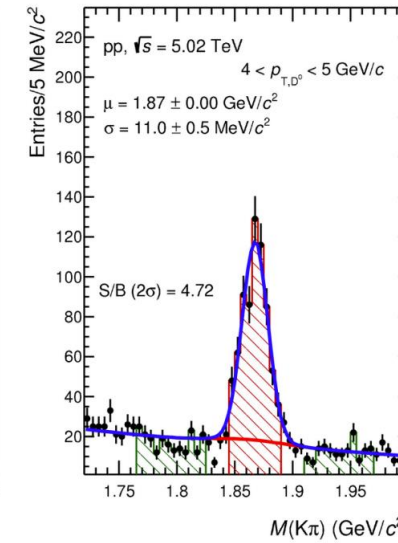
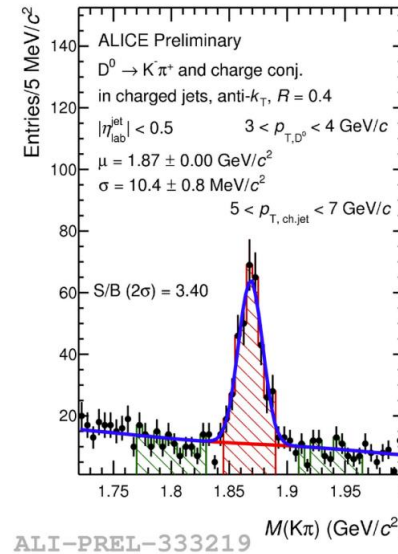


# Analysis method

- Invariant mass distributions of  $k^\pm \pi^\mp$  fitted in bins of  $p_{T,D}$
- Fitting performed with a Gaussian (signal) and an Exponential (background) function

$$Ax^B + Ce^{-\left(\frac{x-m}{2\sigma}\right)^2}$$

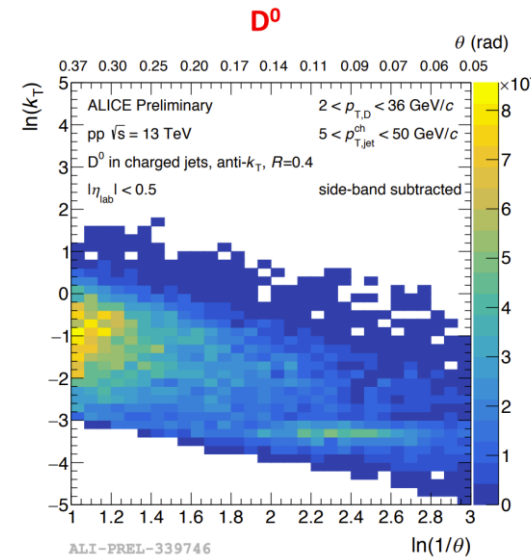
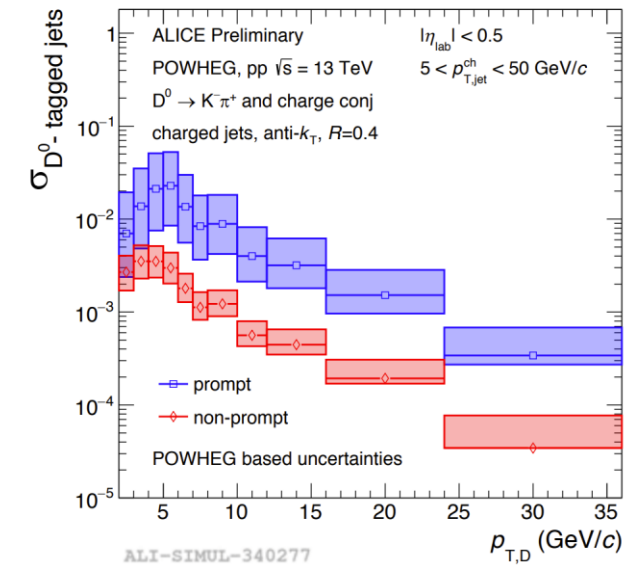
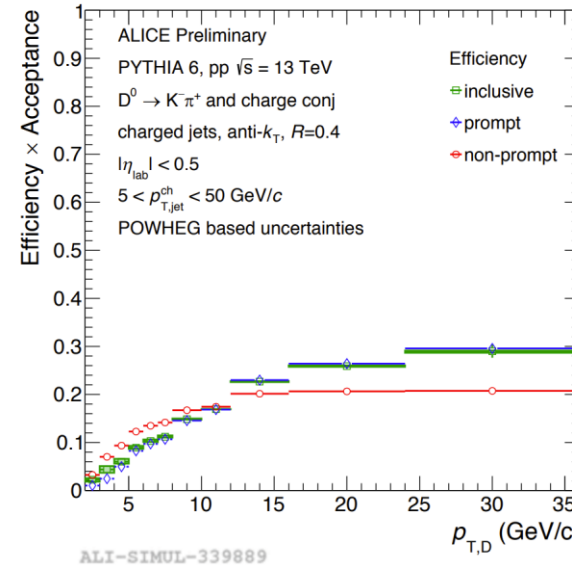
- A side-band subtraction technique is used to extract the signal
- Signal region is  $\pm 2\sigma$  from the peak
- Side-band regions are 4-9 $\sigma$  away from the peak in either direction
- The area of the side-band region is scaled to the area of the background under the peak
- The scaled side-band contribution is subtracted from the signal region to obtain the signal only distribution



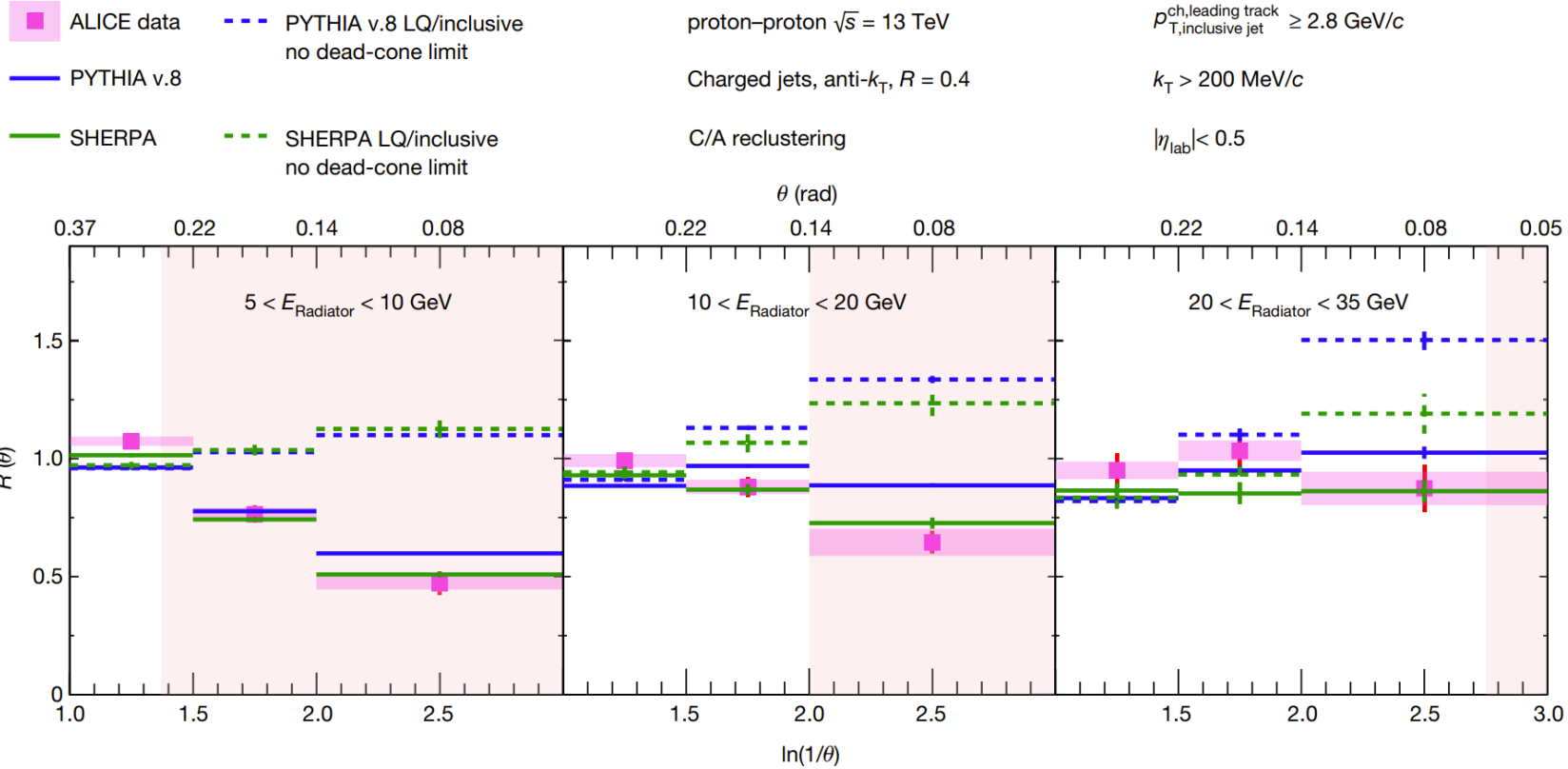
Horizontal band : D\* decays

# Analysis method

- The topological and PID cuts used for the  $D^0$  candidate selection have a finite efficiency
- These efficiencies are calculated from MC in bins of  $p_{T,D}$  for charm (prompt) and beauty (non-prompt) initiated  $D^0$  jets separately
- The **prompt** and **non-prompt** efficiencies are weighted according to their  $\sigma$  from POWHEG
- A **final efficiency value** per  $p_{T,D}$  bin representing the correct admixture of **prompt** and **non-prompt**  $D^0$  jets is extracted
- The side-band subtracted distributions (in  $p_{T,D}$  bins) are scaled by the  $D^0$  jet finding efficiency
- Scaled side-band subtracted Lund-Maps are added across  $p_{T,D}$  bins to obtain the final  $D^0$  splittings Lund-Map



# Result



significance

7.7 $\sigma$

3.5 $\sigma$

1.0 $\sigma$

$$R(\theta) = \frac{1}{N^{\text{D}^0 \text{ jets}}} \frac{dn^{\text{D}^0 \text{ jets}}}{d\ln(1/\theta)} \bigg/ \frac{1}{N^{\text{inclusive jets}}} \frac{dn^{\text{inclusive jets}}}{d\ln(1/\theta)} \bigg|_{k_T, E_{\text{Radiator}}}$$

$$R(\theta)_{\text{no dead-cone limit}} = \frac{1}{N^{\text{LQ jets}}} \frac{dn^{\text{LQ jets}}}{d\ln(1/\theta)} \bigg/ \frac{1}{N^{\text{inclusive jets}}} \frac{dn^{\text{inclusive jets}}}{d\ln(1/\theta)} \bigg|_{k_T, E_{\text{Radiator}}}$$

# Conclusion

- 使用jet declustering 首次在高能对撞物理实验中直接观测到了dead-cone effect。
- Dead-cone effect是QCD的一个基本性质，测量该效应可以验证QCD理论。
- 夸克的质量作为标准模型中的一个重要参数，由于夸克禁闭的存在难以直接测量。而通过测量c夸克的dead-cone effect，可以获得c夸克在强子化之前的质量信息。
- 接下来可以通过测量b强子的dead-cone effect，来探究其质量依赖。也可以测量重离子碰撞中的dead-cone effect来研究介质中的QCD辐射。

**Thanks for listening**

**BACK UP**

The dead cone effect is a prediction of QCD, the theory of strong interactions within the Standard Model of particle physics. It originates from the radiation pattern off a heavy quark as obtained in perturbation theory [1, 2]. For an energetic heavy quark  $Q$  of mass  $M_Q$  and energy  $E_Q$  such that  $E_Q/M_Q \gg 1$ , the gluon emission probability for small emission angle  $\Theta$  and low energy  $\omega$ , can be written as

$$d\sigma_{Q \rightarrow Q+g} \simeq \frac{\alpha_s}{\pi} C_F \frac{\Theta^2 d\Theta^2}{(\Theta^2 + \Theta_0^2)^2} \frac{d\omega}{\omega}, \quad (1)$$

with angular cut-off  $\Theta_0 = M_Q/E_Q$ ;  $\alpha_s$  denotes the strong coupling constant and  $C_F$  the QCD colour factor at the branching vertex  $Q \rightarrow Q + g$ . Therefore, for smaller emission angles  $\Theta < \Theta_0$ , gluon radiation is suppressed and vanishes in the forward direction such that the region with the gluon depopulated cone around the flight direction of the heavy quark  $Q$  is called “dead cone”. For large emission angles  $\Theta \gg \Theta_0$ , the gluon radiation pattern becomes identical to that of a light quark jet, and the same statement holds for the internal angular ordered structure of secondary gluon subjects.

arXiv:2303.13343 [hep-ph]

# Back up

the dead-cone angles in each  $E_{\text{Radiator}}$  interval,  $\theta_{\text{dc}} < m_Q/E_{\text{Radiator}}$ , where emissions are suppressed. For a charm-quark mass  $m_Q = 1.275 \text{ GeV}/c^2$  (ref. <sup>1</sup>), these angles correspond to  $\ln(1/\theta_{\text{dc}}) \geq 1.37, 2$  and  $2.75$  for the intervals  $5 < E_{\text{Radiator}} < 10 \text{ GeV}$ ,  $10 < E_{\text{Radiator}} < 20 \text{ GeV}$  and  $20 < E_{\text{Radiator}} < 35 \text{ GeV}$ ,

and  $20 < E_{\text{Radiator}} < 35 \text{ GeV}$  intervals. It was verified through the MC simulations that non-prompt  $D^0$ -meson tagged jets should exhibit a smaller suppression at small angles in  $R(\theta)$  compared with inclusive jets than their prompt counterparts. This is due to the additional decay products accompanying non-prompt  $D^0$ -meson tagged jets that are produced in the decay of the beauty hadron. These may populate the dead-cone region, leading to a smaller observed suppression in  $R(\theta)$ , despite the larger dead-cone angle of the heavier beauty quark.

Majority of QCD branching is soft & collinear, with following divergences:

$$[dk_j] |M_{g \rightarrow g_i g_j}^2(k_j)| \simeq \frac{2\alpha_s C_A}{\pi} \frac{dE_j}{\min(E_i, E_j)} \frac{d\theta_{ij}}{\theta_{ij}}, \quad (E_j \ll E_i, \theta_{ij} \ll 1).$$

To invert branching process, take pair with strongest divergence between them — they're the most *likely* to belong together.

1. Decluster the current object to produce two pseudojets,  $p_a$  and  $p_b$ , labelled such that  $p_{ta} > p_{tb}$ , where  $p_{ti}$  is the transverse momentum of  $i$  with respect to the colliding beams. We will consider  $p_b$  to be the emission and  $p_a + p_b$  to be the emitter. In the limit where  $p_b$  carries little momentum relative to  $p_a$ ,  $p_a + p_b$  and  $p_a$  can be thought of being the same particle, simply differing through the loss of a small amount of momentum by the radiation of a gluon  $p_b$ .
2. Determine a number of variables associated with the declustering, e.g.

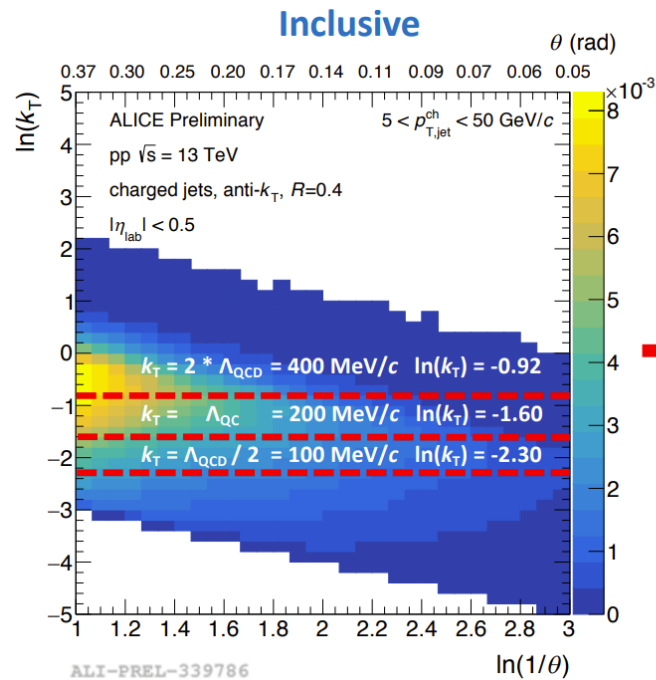
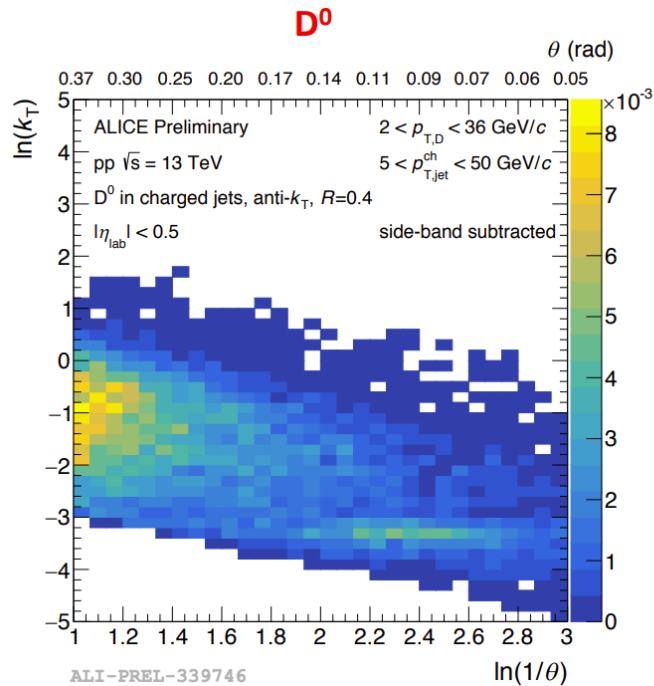
$$\Delta \equiv \Delta_{ab}, \quad k_t \equiv p_{tb}\Delta_{ab}, \quad m^2 \equiv (p_a + p_b)^2, \quad (2.1a)$$

$$z \equiv \frac{p_{tb}}{p_{ta} + p_{tb}}, \quad \kappa \equiv z\Delta, \quad \psi \equiv \tan^{-1} \frac{y_b - y_a}{\phi_b - \phi_a}, \quad (2.1b)$$

In the limit  $p_{tb} \ll p_{ta}$  and  $\Delta \ll 1$ ,  $k_t$  is the transverse momentum of particle  $b$  (the emission) relative to its emitter,  $\psi$  is an azimuthal angle around the (sub)jet axis, and  $z$  is the momentum fraction of the branching. In our default definition of the Lund plane, the coordinates associated with this declustering will be  $\ln \Delta$  and  $\ln k_t$ . One may also, however, make other choices of coordinates, such as for example  $\ln \Delta$  and  $\ln \kappa$ , or  $\ln \Delta$  and  $\ln k_t/p_{t,\text{jet}}$  (with  $p_{t,\text{jet}}$  the jet transverse momentum). We will denote the variables as a tuple  $\mathcal{T}^{(i)} = \{k_t^{(i)}, \Delta^{(i)}, \dots\}$  for the  $i^{\text{th}}$  iteration of this step.

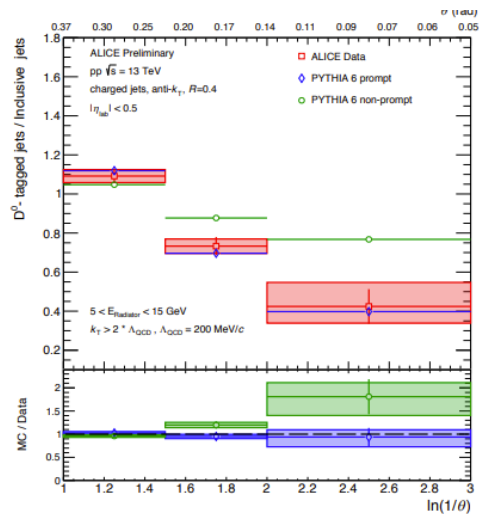
3. Repeat the procedure by going to step 1 for the harder branch,  $p_a$ .

# Back up

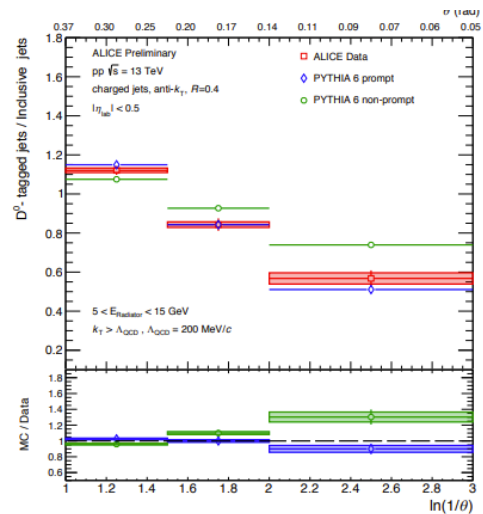


- ❖ Minimum  $k_T$  cuts for splittings are imposed to reduce hadronisation effects
- ❖ Expect to see a stronger suppression for stricter cuts of  $k_T$
- ❖ Stricter  $k_T$  cuts come at a cost to statistics

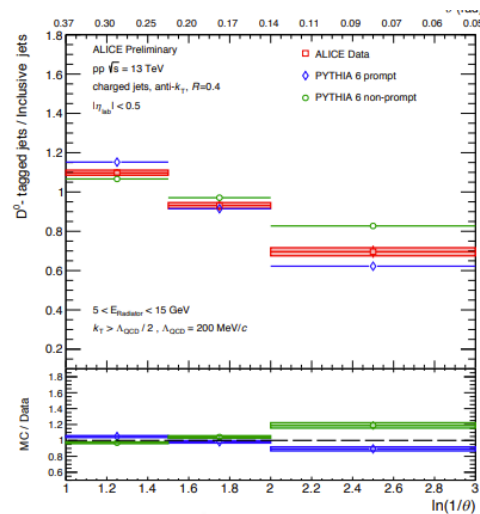
- ❖ Each splitting in the inclusive jet sample has a leading track requirement of  $p_T > 2.8 \text{ GeV}/c$  corresponding to the minimum  $m_{T,D}$



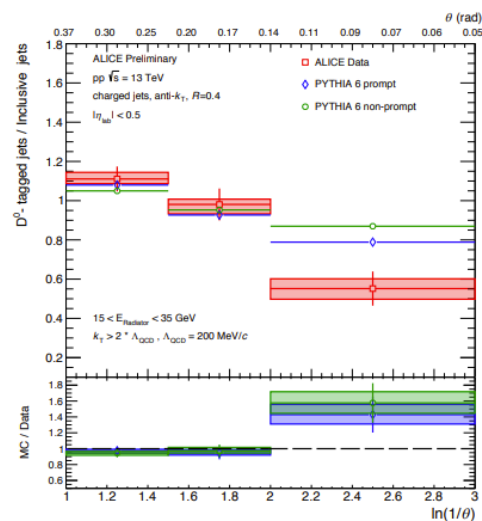
ALI-PREL-341301



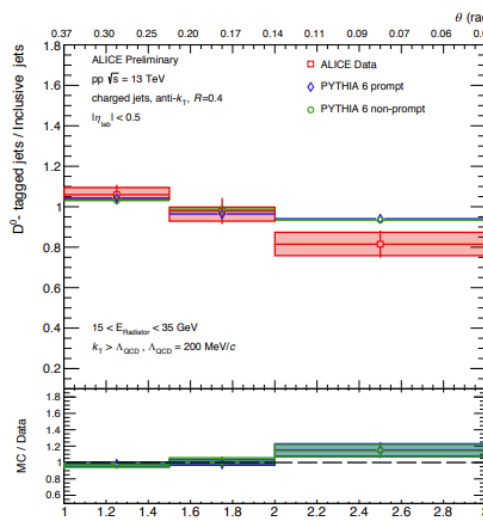
ALI-PREL-341306



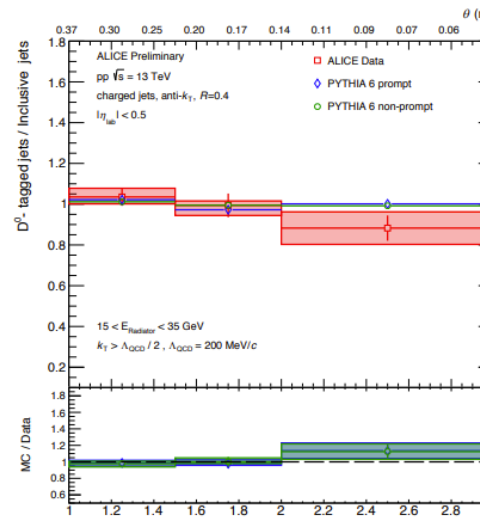
ALI-PREL-341311



ALI-PREL-341316



ALI-PREL-341321



ALI-PREL-341326

- ◆ Fully non-prompt PYTHIA shows much less suppression compared to prompt PYTHIA at low energies
- ◆ Additional decay products of the beauty-hadron cloud the dead-cone region

# Back up

## ➤ Sources of systematic uncertainty for $D^0$ jets :

- ❖ Fitting variations
- ❖ Cut variations
- ❖ Side-band variations
- ❖ POWHEG variations
- ❖ Tracking Efficiency

## ➤ Sources of systematic uncertainty for inclusive jets :

- ❖ Min  $p_T$  cut on hardest track in leading splitting prong varied
- ❖ Tracking Efficiency

The 2D unfolding of the Lundplane is beyond the scope of this analysis, as matching different stages of the splitting history at truth and detector level is poorly defined. Therefore the final reported observable will be a detector

**Table 1 |  $R(\theta)$  systematic uncertainties**

Source	$E_{\text{Radiator}}$		
	5–10 GeV	10–20 GeV	20–35 GeV
Invariant-mass fitting	2.3	1.4	3.0
Side-band subtraction	2.0	1.8	1.4
$D^0$ -jet selection stability	4.1	5.0	7.2
Non-prompt contribution	1.0	3.5	1.1
Leading hadron $p_T$ selection	2.0	3.2	0.2
Detector effects	0.7	5.2	0.9
Total	5.6	8.9	8.1

The percentage magnitude of the systematic uncertainties of each source considered, and the total systematic uncertainty, for the  $R(\theta)$  variable are shown for the smallest splitting-angle interval  $2 \leq \ln(1/\theta) < 3$ .